minerals

MDPI

Article

Multistage Adsorption-Elution Process for Efficient Separation and Purification of Dysprosium and Neodymium from Acidic Solution Using Functionalized Resins

Fakhri Ali Salem Mohammed and Yahui Zhang *

Department of Process Engineering, Memorial University of Newfoundland, St John's, NL A1B 3X5, Canada; fasmohammed@mun.ca

* Correspondence: yahuiz@mun.ca

Abstract

Neodymium (Nd) and dysprosium (Dy) are two critical rare earth elements for fabricating NdFeB permanent magnets, which have crucial applications in modern technologies. The increasing global demand for Nd and Dy emphasizes new efficient processes for their recovery and purification, which are technologically challenging due to their close physical and chemical properties. Through systematic exploration, it was found that Lewatit VP OC 1026 resin impregnated with di-(2-ethylhexyl) phosphoric acid (D2EHPA) had a strong adsorption preference for Dy^{3+} over Nd^{3+}, which is highly suitable for Dy-Nd separation from their mixed solutions under optimized conditions. The loaded resin could be eluted using dilute sulfuric solutions for recycling to the adsorption process. By employing a multistage adsorption-elution process analogous to distillation, efficient Dy-Nd separation and purification were realized from their mixed solution, with a prospective purity of 99.13% and recovery of 97.45% for Dy and a prospective purity over 99.96% and recovery of above 99.90% for Nd, despite the large concentration disparity between Dy and Nd, where Nd concentration is over 26 times that of Dy. This research demonstrates that efficient recovery and purification of metals from aqueous solutions can be achieved using selective resin adsorption processes analogous to distillation, despite large concentration differences of the metals in the solutions, which presents new alternative approaches.

Keywords: neodymium (Nd); dysprosium (Dy); recovering; purifying; selective ion exchange; multistage adsorption-elution process; analogous to distillation

Check for updates

Academic Editor: Kenneth N. Han

Received: 10 June 2026
Revised: 23 July 2026
Accepted: 27 July 2026
Published: 30 July 2026

Copyright: © 2026 by the authors. Licensee MDPI, Basel, Switzerland. This article is an open access article distributed under the terms and conditions of the Creative Commons Attribution (CC BY) license.

1. Introduction

Neodymium (Nd) and dysprosium (Dy) are two critical rare earth elements (REEs) for fabricating NdFeB permanent magnets, which are the strongest magnetic materials having crucial applications in modern technologies [1,2], including electric vehicles [3], green energy (e.g., wind turbines [4]), and advanced electronics due to their high magnetic strength and energy efficiency [5,6]. Nd provides strong magnetic properties, while Dy enhances thermal stability and resistance to demagnetization at elevated temperatures [7]. The increasing demand for clean energy technologies has significantly emphasized the importance of Nd and Dy, making their efficient recovery and purification, particularly from end-of-life NdFeB magnets and electrical/electronic equipment, vital to ensuring a sustainable supply and reducing dependence on primary resources, given the high contents of REEs in these spent products. Obviously, the available selective separation processes for

recovering earth elements are both technologically and chemically challenging due to their similar physical and chemical properties, as exhibited in the periodic table [8,9]. Thus, it is crucial to develop efficient, selective methods for recovering and reusing these critical metals. Various technological routes are explored: co-precipitation, the electrochemical method, membrane technology, biosorption processes, conventional solvent extraction, and ion exchange [10–14]. The precipitation process used to separate the REEs involves direct precipitation with hydrogen fluoride or oxalic acid [15–17] or double salt precipitation at varying pH values [18,19]. The main restrictions of the precipitation methods are attributed to the high level of chemical consumption and to the high loss of REEs [20,21]. Conventional solvent extractions are commonly used methods, despite existing disadvantages, including high solvent consumption, high waste volumes, limited selectivity under acidic conditions, and hazardous environmental impacts [22–27].

Ion exchange processes are solid–liquid separation techniques that employ polymeric resins functionalized with active groups and serving as the solid phase, which can selectively bind specific ionic species usually dissolved in solution [28,29]. Ion exchange offers several advantages over conventional solvent extraction, including superior selectivity and exceptionally high adsorption efficiencies [30], often reaching 99.999%, thereby enabling the production of ultra-high-purity REEs. In addition, ion-exchange systems provide simpler operation and handling, enhanced control over process parameters, reduced environmental footprint, and suitability for small-scale applications [13,31,32]. Different studies have been conducted to improve the selective recovery of REEs from leaching solutions of various secondary resources, based on the fundamental principles of ion exchange for rare earth separation. Table 1 summarizes the key functional groups on resins investigated in prior studies to enhance the understanding of resin selectivity and efficiency. These works provide an important basis for understanding the present problems and guide the design of more efficient REE separation and purification strategies. Fila et al. studied the recovery of metal ions (especially REEs and heavy metals) from nickel-metal battery waste using a Diphonix resin functionalized with sulfonic, diphosphonic, and carboxylic multifunctional groups. The results indicate that adsorption was higher with 0.2 M HNO_3, and the affinity of the Diphonix resin for the tested metal ions was determined as La(III) > Pr(III) > Fe(III) > Nd(III) > Ce(III) > Cu(II) > Zn(II) > Co(II) > Ni(II) [33]. In another study, José and Ladeira investigated the recovery of a series of REEs, including La, Pr, Nd, Sm, Eu, Gd, Dy, and Er, using Lewatit® MDS 200H resin functionalized with sulfonic acid groups. The experiments were conducted in a column system at pH 3.5 using a synthetic multi-element solution containing 3000 mg/L REEs, along with 1000 mg/L metal impurities, including Al, Ca, and Mg, and sulfate ions (SO_4^{2-}) to simulate an acid mine drainage matrix. The resin achieved REE loading efficiencies of approximately 85%, while the co-loading of metal impurities was limited to about 30%, indicating preferential adsorption of REEs over the accompanying impurities [34]. In another method, the Purolite C150 and Finex CS16GC, both containing sulfonic acid groups, and the Purolite S940 with aminophosphonic functional groups were used by Virolainen et al. to recover REEs from phosphogypsum by combining leaching and adsorption (i.e., resin-in-leach process). where the resin with aminophosphonic functional groups possessed better loading efficiency, reaching 19.2 g of REEs per 1 kg of resin, than the resin bearing sulfonic acid groups with 5.6 g (REEs)/kg (resin) [35].

The effectiveness of solvent-impregnated resins (SIRs) relies on their superior extraction efficiency, making them highly selective sorbents. These SIRs consist of a polymeric matrix uniformly impregnated with liquid ionic extractants, a design that enhances mass transfer and significantly improves separation performance compared with conventional ion-exchange resins and solvent extraction processes. The Cyanex 272-impregnated Amberlite XAD-7 resin, which contains a phosphinic acid group, was used by Inan et al. to

investigate the extraction and separation of La, Pr, Nd, Sm, Eu, and Gd from a nitric acid solution; the loaded resin reached capacities of 11.1, 0.56, 1.69, 0.75, 0.10, and 0.25 mg g^{-1} for La, Pr, Nd, Sm, Eu, and Gd, respectively, at equilibrium. Complete elution was confirmed for Pr (III), Nd (III), Sm (III), and Gd (III), and an elution rate of 95.1% was achieved for Eu (III) using 0.1 M HNO_3 [36]. Konvalenko and his workers improved the efficiency of the used solvent-impregnated resin through the treatment of styrene–divinylbenzene copolymer (LPS-500) with mixtures of polydentante extractant (2-diphenylphosphoryl)-4-ethylphenoxy)methyl)diphenylphosphine oxide (L) and an ionic liquid $[C4mim]^+[Tf2N]^-$ to recover Nd^{3+} from nitric acid solution. They found the invented SIR containing 40% of a mixture of (L) and $[C4mim]^+[Tf2N]^-$ with a molar ratio of 2:1 exceeded the SIR containing Cyanex 923.

It is notable that the ion-exchange processes provide an effective route for the selective adsorption of REEs, involving the preferential extraction or targeted adsorption of individual elements or specific groups from leaching solutions of various secondary resources. This approach is of considerable importance in both scientific research and industrial applications. Nevertheless, achieving efficient selective separation remains a significant challenge due to the strong similarities in the chemical and physicochemical properties of REEs. These similarities persist despite minor variations in ionic radii and oxidation states, particularly between light and heavy REEs [3,37]. In addition, the uneven distribution and wide concentration ranges of REEs in leach solutions further complicate the separation process, requiring carefully optimized operating conditions and the use of highly selective functional materials, such as tailored ion-exchange resins.

Conventional methods, including solvent extraction and precipitation, have shown limited capability for selective purification and separation of REEs, whereas ion-exchange processes have gained increasing attention as an effective approach for achieving high-purity REEs [14].

In contrast to many previous studies, this research focuses on exploring the selectivity of functional groups (ligands) on the resins towards a specific REE (i.e., Dy or Nd) relative to the other element. This study uses Lewatit VP OC 1026 resin functionalized (impregnated) with di-(2-ethylhexyl) phosphoric acid (D2EHPA) to selectively separate dysprosium from a solution where the neodymium concentration is 26 times higher (see Section 2.2), employing a multistage adsorption-elution process that mimics distillation. The separation strategy is based on the differential affinity of the selected resin for the REEs, specifically the weaker interaction of neodymium, a light REE (LREE), compared with the stronger adsorption of dysprosium, a heavy REE (HREE). This behavior is primarily attributed to differences in ionic radii across the lanthanide series, where the smaller ionic radii of heavy rare earth elements result in higher charge density and stronger interactions with functional groups, thereby facilitating selective separation [3,34,36].

Table 1. Summary of selected studies on desorption of REEs and regeneration of exhausted resins for REE recovery.

Function Group	Resin	REE Recovery Process					Performance of the Process	Ref
		Target Element	Operation Parameter					
			T (°C)	pH	Time (min)	Elution Process		
phosphonic and sulfonic functional groups	Purolite S957	La^{3+}, Ce^{3+}, Nd^{3+}, Fe^{3+}, Ni^{2+}, Cu^{2+}, Co^{2+}, and Zn^{2+}	Room temp.	0.2 M HNO_3	60	The best desorption was at 2.0 M of HNO_3 or HCl	Purolite S957 showed higher affinity for trivalent ions La^{3+}, Ce^{3+}, Nd^{3+}, and Fe^{3+}, than for divalent ions Cu^{2+}, Co^{2+}, and Zn^{2+}	[38]

Table 1. *Cont.*

Function Group	Resin	REE Recovery Process					Performance of the Process	Ref
		Target Element	Operation Parameter					
			T (°C)	pH	Time (min)	Elution Process		
Sulfonic (Na^+ form) Sulfonic (H^+ form) Bis(2-pyridylmethyl)amine (bis-picolylamine)	Amberlite 200C Na, Amberlite 200C H Dowex M 4195	La^{3+}, Ce^{3+}, Nd^{3+}	20 and 60	2.5	120	2.0 M of HNO_3 or HCl, HNO_3 showed better efficiency	Amberlite200C Na and H, showed very good potential for the removal of REEs from acidic solution; Dowex M4195 has lower sorption capacity compared to Amberlite towards REEs.	[39]
Sulfonic Acid	Dowex 50WX8	Pr^{3+}, Dy^{3+}, and Y^{3+}	Room temp	------	60	58% of pr with 1.0 M citric acid55% Dy with 1.0 M nitric acid 56% Y with 1.0 M $CH_2O_3.2H_3N$	30.0 mg/g for Pr^{3+}, 50 mg/g for Dy^{3+}, and 60 mg/g for Y^{3+}.	[40]
Sulfonic groups	Strongly cation resin (SQS-6)	La^{3+}, Nd^{3+}	25	4.0	10	HF + HCl	13.8 mg/g for La^{3+}, 12.7 mg/g for Nd^{3+}.	[41]
Sulfonic group	D72 Microporous resin	Y^{3+}, Ce^{3+}, La^{3+}, Nd^{3+}, Gd^{3+}, and Dy^{3+}	25	-------	-------	1.7 mol/L HNO_3 8.0 mol/L NH_4NO_3 + 0.2 mol/L HNO_3	REE adsorption capacity 001 × 7 = 0.9950 mg/cm^3, 005 × 8 = 0.7794 mg/cm^3, D72 = 2.4648 mg/cm^3.	[42]
Phosphinic acid	Cyanex 272 impregnated Amberlite XAD-7 resin	La^{3+}, Pr^{3+}, Nd^{3+}, Sm^{3+}, Eu^{3+}, Gd^{3+}	25	2.4	180	0.01 M HNO_3 or 0.01 M HCl	The adsorption of Gd > Eu > Sm > Nd > Pr > La	[36]
Carboxylic acid	Acrylic resin (110 resin)	Nd^{3+}	25	6.0	3600	3.0 M HCl	308 mg/g, the maximum adsorption capacity	[43]
Aminophosphonic And Aminomethylphosph-onic	Amberlite IRC-747 and Lewatit TP-260	La^{3+}, Nd^{3+}, Gd^{3+}, Dy^{3+}, Er^{3+}, Yb^{3+}, Sc^{3+}, and Y^{3+}	50	----	180	9 M and 18 M of H_2SO_4 or Na_2CO_3 1M	1.8 mg/g dry resin, the maximum capacity	[21]
Carboxylic acid	(RTPA) Resorcinol-tereph-thalaldehyde	La^{3+}, Nd^{3+}, Eu^{3+}, Dy^{3+}, Yb^{3+}	25	4.7	60	2.0 M HNO_3	Higher than 50 mg/g	[13]

2. Experiments

2.1. Materials and Instruments

All chemicals used were of analytical reagent (A.R.) grade. A neodymium (III) sulfate hydrate solution (6000 mg/L of Nd) was prepared using 99.9% pure neodymium (III) sulfate hydrate (Sigma-Aldrich, Oakville, ON, Canada, Catalogue #: 325813-50G), while dysprosium sulfate (ProChem Inc., Rockford, IL, USA) was used to prepare a 200 mg/L of Dy solution. The pH was adjusted using 1 M hydrochloric acid, which was prepared by diluting 37% HCl (Fisher Scientific, Toronto, ON, Canada, Catalogue #: A144S-212). Deionized (DI) water, further purified using a Millipore Milli-Q water purification system, was used to prepare solutions throughout the experiments. The study aims to assess the adsorption efficiency and selectivity of the selected cationic exchange resins, which consist of 14 different functional groups, as detailed in Table 2. The collected solution samples were analyzed using Inductively Coupled Plasma Optical Emission Spectroscopy (ICP-OES), Santa Clara, USA. We measured the pH using a Thermo Scientific Orion Star A111 pH meter, Ottawa, ON, Canada. A platform shaker (Promax 2020, Heidolph Instruments GmbH &

Co. KG, Schwabach, Germany) and an incubator shaker (InnovaR 43, New Brunswick Scientific, Canada) were used for adsorption tests.

Table 2. Resins tested in this study.

Functional Groups	Ion Exchange Resin	Reference
Amidoxime	Puromet MTS 9100	[44]
Aminophosphonic	ResinTech SIR 500	[45]
	Purolite S950plus	[46]
	Purolite S940	[47]
	Puromet MTS9500	[48]
Phosphonic and sulfonic acid	Purolite MTS 9570	[49]
Sulfonic acid	Dowex G-26	[50]
	Amberlite IRC-120	[51]
Di-2-ethylhexylphosphat (D2EHPA)	Lewatit vp oc 1026	[52]
	Purolite MTX7010	[53]
Aminomethyl-phosphonic acid	Lewatit MDS TP 260	[54]
Sulfonic acid (strong acid cation)/Trimethyl-ammonium(strong base anion)	Amberlite IRN-150	[55]
Bis-(2,4,4-trimethylpentyl)phosphinic acid	Lewatit® TP 272	[56]
Iminodiacetic	Purolite MTS9300	[57]
	Purolite S930 Plus	[58]
	Lewatit monoplus TP207	[59]
	Lewatit monoplus TP208	[60]
	Purolite S930	[61]
Thiourea	PuroliteMTS9140	[62]
	Lewatit monoplusTP214	[63]
Aluminosilicate	ResinTech SIR-600	[64]
Isothiouronium	Puromet MTS9200	[65]
Thiol chelating resins	Puromet MTS9240	[66]
Carboxylic acid	DOWEX™ MAC-3	[67]

2.2. Sample Preparation

Three different aqueous solutions were prepared for resin adsorption tests. The first single solution was prepared by dissolving the appropriate amount of dysprosium sulfate ($Dy_2(SO_4)_3.8H_2O$) in 1000 mL of deionized water to yield a solution with around 200 mg/L Dy. And the second single solution was prepared by dissolving the appropriate weight of neodymium (III) sulfate hydrate ($Nd_2(SO_4)_3 \cdot xH_2O$) to obtain a 1000 mL solution containing about 6000 mg/L of Nd. The third solution is a binary solution, prepared by dissolving the required amounts of dysprosium sulfate and neodymium (III) sulfate hydrate, resulting in anticipated concentrations. The synthetic binary solution mimics a leach liquor from which iron ions have already been selectively removed in a prior processing step as described in reference [14]. The pH of all solutions was adjusted using 1 M hydrochloric acid diluted from 37% HCl using deionized water.

2.3. Resin Preparation

As the first step, all resins used in the experiments were activated to achieve uniformity, remove impurities or preservatives, open active sites, ensure consistent performance, and hydrate or swell the resin. This pre-conditioning involved treating the appropriate amount of resin with 20 mL of 30% (v/v) HCl and shaking on a platform shaker (Promax 2020, Heidolph Instruments GmbH & Co. KG) at 150 rpm for 24 h, followed by filtration. The resins were washed with deionized water while continuously shaken at 150 rpm for 1 h, then filtered. Finally, the resins were dried to a constant weight at room temperature for later resin adsorption tests.

2.4. Characterization of the Adsorption

Batch adsorption experiments were conducted on single-metal solutions containing Nd^{3+} or Dy^{3+} to evaluate various resins across 14 functional groups (see Table 2). A most promising resin, Lewatit VP OC 1026, impregnated with di-(2-ethylhexyl) phosphoric acid (D2EHPA), was then tested with a Nd-Dy binary solution, in which the initial pH was adjusted to 0.67 using 1 M HCl. Various resin dosages (0.05, 0.1, 0.15, 0.2, and 0.3 g/mL) were tested, with each sample contacting 20 mL of solution in a 50 mL Erlenmeyer flask under batch conditions. The mixtures were agitated on a reciprocating shaker at 150 rpm for 60 min at ambient temperature unless otherwise specified. The resins remained stably dispersed as monodisperse spherical beads throughout the experiments, with no visible particle agglomeration or clotting observed under the tested hydrodynamic conditions (150 rpm).

Figure 1a,b illustrates the adsorption and desorption mechanisms of rare earth element ions on cation-exchange resins bearing acidic functional groups. The adsorption (ion-exchange) of Nd^{3+} and Dy^{3+} ions onto cation-exchange resins can be represented by the general chemical reactions shown in Equations (1) and (2), respectively, in which the protons in the resin's functional groups are replaced by the trivalent rare earth cations. Meanwhile, in the desorption step, the REE-loaded resin is treated with a strong acid (e.g., HCl or H_2SO_4), which supplies a high concentration of H^+ ions. These protons compete with the bound metal ions, reversing the ion-exchange reaction and releasing the adsorbed REEs back into solution.

$$Nd^{3+}_{(aq)} + 3R - XH_{(s)} \rightarrow (R - X)_3Nd_{(s)} + 3H^+_{(aq)} \quad (1)$$

$$Dy^{3+}_{(aq)} + 3R - XH_{(s)} \rightarrow (R - X)_3Dy_{(s)} + 3H^+_{(aq)} \quad (2)$$

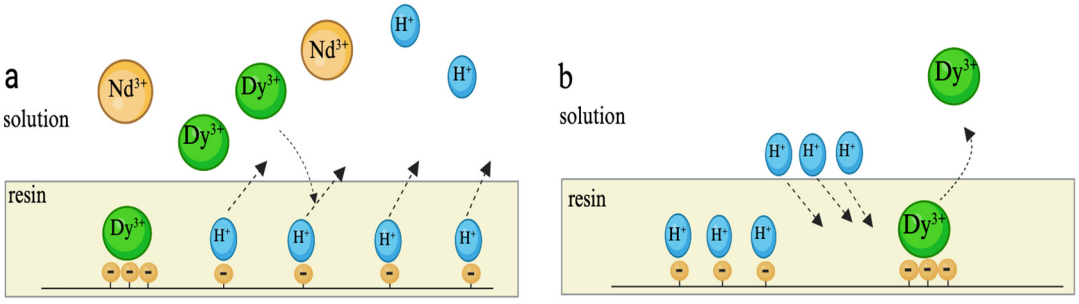


Figure 1. REE's adsorption (**a**) and elution (**b**) mechanisms.

Considering that the resin (denoted as R–H) contains protonated functional groups and REE^{3+} represents Nd^{3+} and Dy^{3+} ions, the adsorption of REEs primarily proceeds through an ion-exchange mechanism in which protons are replaced by trivalent metal ions. The adsorption efficiency (R%) of Nd^{3+} or Dy^{3+} at equilibrium, as expressed in Equation (3),

and the corresponding equilibrium ion-exchange capacity of the resin (mg/g), given in Equation (4), were determined using the following relationships:

$$R\% = ((C_0 - C_e)/C_0) * 100\% \quad (3)$$

$$q_e = (C_0 - C_e) * V/m \quad (4)$$

where q_e denotes the adsorption capacity of the polymeric resin toward Nd^{3+} or Dy^{3+} ions at equilibrium. The parameters C_0 and C_e represent the initial and equilibrium concentrations of Nd^{3+} or Dy^{3+} ions in the aqueous solution (mg/L), respectively. Furthermore, V corresponds to the solution volume (0.02 L here), while m represents the mass of the polymeric resin used in the adsorption process (g).

The elution efficiency, representing the recovery percentage of metals in the eluted (or washing) solution, was determined based on the analyzed metal concentrations using a calculation approach similar to that employed for R%. The calculated elution percentages describe the fraction of metal recovered during the current elution stage.

The prospective purity (pp%) of Nd^{3+} or Dy^{3+} was determined using Equation (5):

$$pp\% = \left(\frac{C_1}{C_1 + C_2}\right) * 100\% \quad (5)$$

where C_1 and C_2 correspond to the concentrations of metal 1 (e.g., Nd^{3+} or Dy^{3+}) and metal 2 (e.g., Nd^{3+} or Dy^{3+}), respectively, in the purified solution with a defined volume V_p (0.020 L in this study). The purified Dy or Nd solution could subsequently be concentrated through the resin adsorption-elution process followed by electrowinning.

The metal recovery in the purified solution with volume V_p was calculated according to Equation (6):

$$recovery\% = (C/C_{start}) * 100\% \quad (6)$$

where C represents the metal concentration in the purified solution, while C_{start} refers to the initial metal concentration prior to purification within the same solution volume V_p.

3. Results and Discussion

The resin adsorption test arrangements are shown in Figure 2. The first test stage aimed to evaluate the performance of different commercial resins for adsorbing Nd^{3+} and Dy^{3+} ions from single metal solutions. Based on the experiment results, the resins with effective functional groups were selected for subsequent tests. In the second stage, the selected resins were tested for the separation of Nd^{3+} and Dy^{3+} from a binary solution. Finally, the most efficient resins with selective functional groups were evaluated to determine the optimal operating conditions, including resin dosage, solution pH, operating temperature, adsorption time, and shaking speed.

3.1. Adsorption Efficiencies for Nd and Dy from Single Metal Solutions Using Various Resins

3.1.1. Explored Resins Bearing Functional Groups with Low Bonding Capacity for Nd and Dy

A thorough investigation was carried out on several resins, including Puromet MTS 9100 with an amidoxime functional group; Lewatit® TP 272 containing Bis-(2,4,4-trimethylpentyl)phosphinic acid; Puromet MTS 9300, Purolite S930 PLUS, Lewatit® MonoPlus TP 207, Lewatit® MonoPlus TP 208, and Purolite S930, all bearing iminodiacetic groups; Puromet MTS 9140 and Lewatit MonoPlus TP 214 resins with thiourea groups; SIR-600 containing aluminosilicate; Puromet MTS 9200 having an isothiouronium functional group; and DOWEX™ MAC-3 possessing carboxylic acid groups. All the tested resins

demonstrated relatively low adsorption capacities for dysprosium (Dy^{3+}) and neodymium (Nd^{3+}), with adsorption efficiencies below 15%, as shown in Table 3. Clearly, the limited adsorption capacity indicates that these resins have poor affinity or weaker interactions between their functional groups and the Dy^{3+} and Nd^{3+} ions, restricting their effectiveness in adsorbing these REEs.

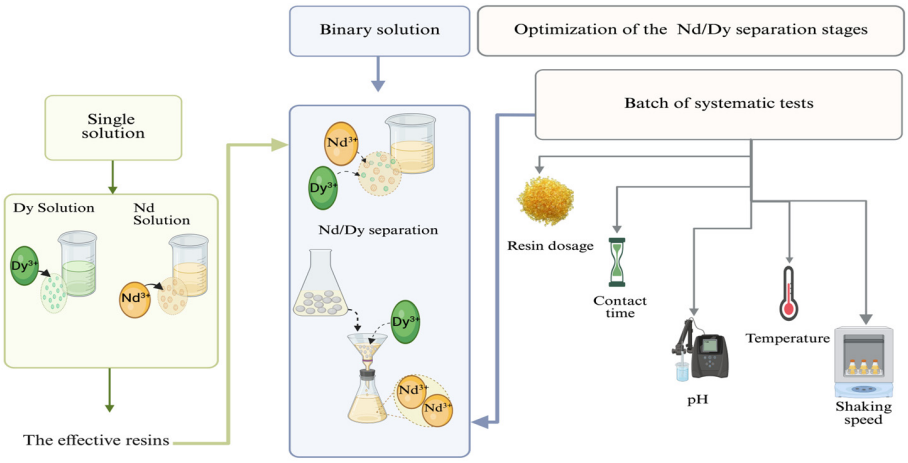


Figure 2. Resin adsorption test protocol for the separation of neodymium and dysprosium.

Table 3. Summary of resins with lower adsorption efficiency at resin dosages of 0.05 g/mL and 0.30 g/mL.

Functional Group	Commercial Resins	Dy Dosage (g/mL)	Dy R%	Nd Dosage (g/mL)	Nd R%
Amidoxime	Puromet MTS 9100	0.05	9.50	0.05	0.24
		0.30	14.13	0.30	8.77
Bis-(2,4,4-trimethylpentyl)phosphinic acid	Lewatit® TP 272	0.05	1.02	0.05	0.01
		0.30	3.48	0.30	1.88
Iminodiacetic	Puromet MTS9300	0.05	0.90	0.05	0.60
		0.30	3.73	0.30	11.23
	Purolite S930 PLUS	0.05	3.09	0.05	0.43
		0.30	7.97	0.30	4.63
	Lewatit® MonoPlus TP 207	0.05	3.72	0.05	0.15
		0.30	10.11	0.30	6.47
	Lewatit® MonoPlus TP 208	0.05	1.31	0.05	0.25
		0.30	6.25	0.30	1.90
	Purolite S930	0.05	4.30	0.05	0.02
		0.30	11.77	0.30	2.31
Thiourea	Puromet MTS9140	0.05	0.33	0.05	0.58
		0.30	6.71	0.30	2.72
	Lewatit® MonoPlus TP 214	0.05	7.36	0.05	0.02
		0.30	14.17	0.30	9.82
Aluminosilicate	SIR-600	0.05	2.31	0.05	4.23
		0.30	7.71	0.30	13.21
Isothiouronium	Puromet MTS9200	0.05	2.25	0.05	1.02
		0.30	11.49	0.30	13.30
Carboxylic acid	DOWEX™ MAC-3	0.05	1.72	0.05	0.10
		0.30	5.67	0.30	0.93

3.1.2. Finding Resins with High Adsorption Efficiencies for Nd or Dy from a Single Metal Solution

Resins with Aminophosphonic Functional Groups

Four resins containing aminophosphonic functional groups, i.e., ResinTech SIR-500, Purolite S950 PLUS, Purolite S940, and Puromet MTS9500, were tested for their ability to adsorb neodymium or dysprosium ions from two separate single metal solutions: one containing neodymium and the other with dysprosium. It can be observed that all resins exhibit a high absorption capacity for dysprosium, which increases with higher resin dosages due to more available active exchange sites.

As shown in Figure 3a, both S950 PLUS and S940 resins demonstrated higher adsorption efficiencies for Dy at lower resin dosages compared with MTS9500 and SIR-500. Both S950 PLUS and S940 quickly reached near-maximum efficiency, achieving values close to 99.8% at a resin dosage of 0.15 g/mL, which were maintained at higher dosages. This plateau indicates early saturation and a strong affinity for Dy^{3+}; in contrast, SIR-500 and MTS-9500 showed a relatively gradual increase, starting around 93% at a 0.05 g/mL resin dosage and continuing to increase over 99% at the highest resin dosage of 0.3 g/mL. Overall, resins with aminophosphonic functional groups demonstrated a significant adsorption capacity of Dy^{3+} due to their strong affinity for Dy^{3+}.

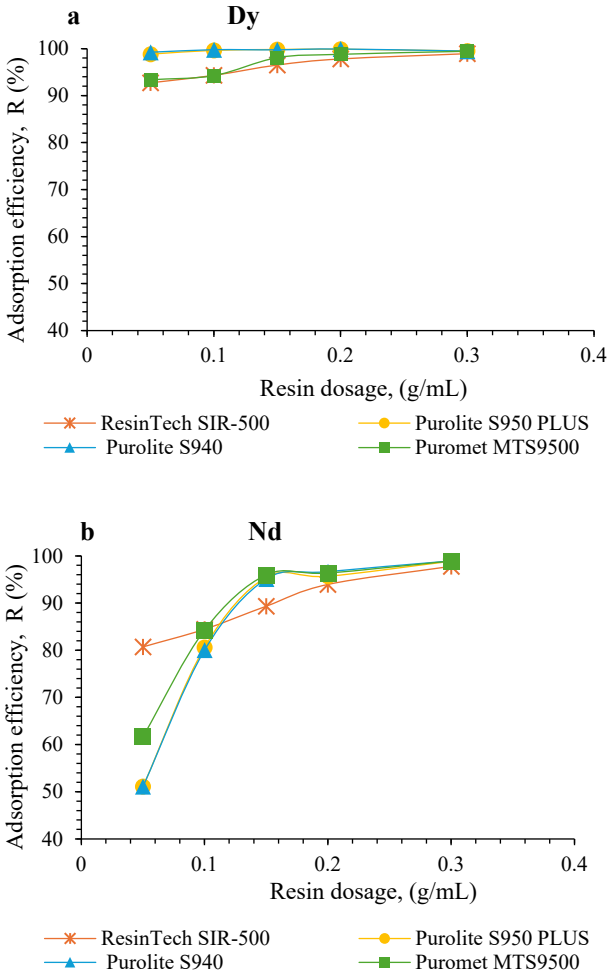


Figure 3. Adsorption efficiencies of Dy^{3+} (**a**) and Nd^{3+} (**b**) using resins containing aminophosphonic functional groups at pH 0.67, 150 rpm, room temperature, and 60 min contact time.

For Nd, the adsorption efficiency increased with resin dosage for all resins as shown in Figure 3b, with some significantly different behavior at low dosages. SIR-500 exhibited

the best performance at the initial resin dosage, reaching over 80% compared to S950 PLUS, S940, and MTS-9500. As the dosage increased to 0.15 g/mL, S950 PLUS, S940, and MTS-9500 showed substantial improvement, reaching over 95%, compared to around 89% for SIR-500. This improvement is attributed to the availability of active binding sites, resulting in a strong adsorption for Nd^{3+}. At high dosage (0.3 g/mL), all resins obtained high adsorption efficiencies ranging from 97% to 99%. Generally, the aminophosphonic functional group exhibited high adsorption affinity for Nd and Dy.

Resins Containing Sulfonic Acid Groups

Figure 4a,b displays the adsorption efficiency of Dy^{3+} and Nd^{3+} ions, respectively, from two separate solutions using the ion-exchange resins Amberlite IRC120 and Dowex G26, both containing sulfonic acid groups, at resin dosages ranging from 0.05 to 0.30 g/mL. Both resins show significant adsorption efficiency for Dy, which increases with resin dosage. At a low dosage (0.05 g/mL), both resins have similar efficiency, reaching 94.25% and 92.96%, respectively. At 0.15 g/mL, Dowex G26 reaches adsorption equilibrium at 99.21%, indicating a strong affinity for Dy.

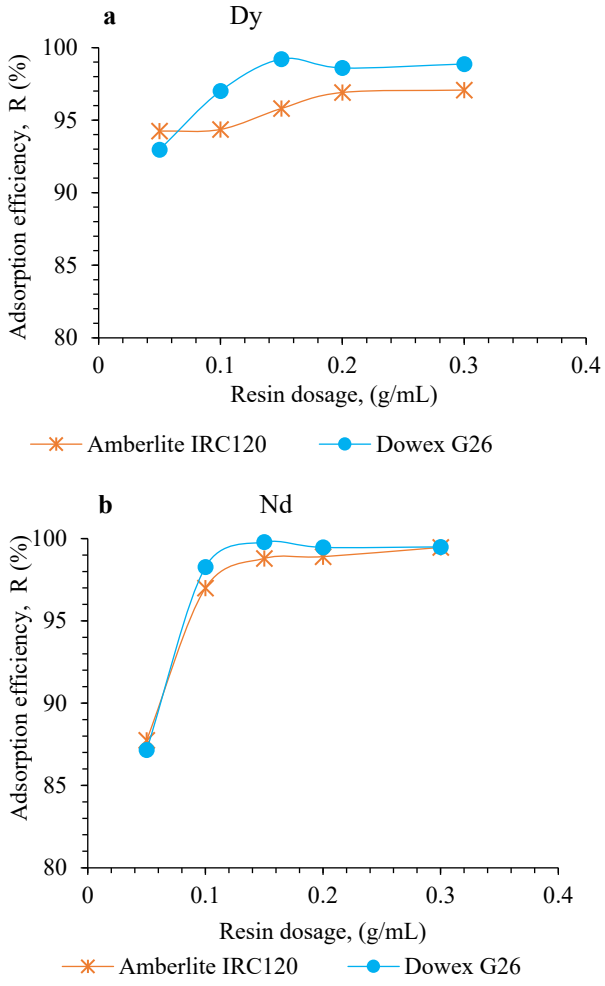


Figure 4. Adsorption efficiencies of Dy (**a**) and Nd (**b**) using Amberlite IRC120 and Dowex G26 with sulfonic acid functional groups at pH 0.67, 150 rpm, room temperature, and 60 min contact time.

Amberlite IRC120 also gradually improves, reaching an adsorption efficiency of 95.81% at the same dosage and continuing to increase at higher dosages (0.3 g/mL), surpassing 97%. Overall, increasing resin dosage improves Dy uptake for both resins.

Figure 4b illustrates how the resin dosage influences Nd^{3+} adsorption efficiency using Amberlite IRC120 and Dowex G26 with sulfonic acid groups. Both resins display similar behavior across all dosages. At the lowest dose (0.05 g/mL), they reach moderate efficiencies of around 87%. When the dose increases to 0.10 g/mL, efficiency rises sharply to 97%–98%, indicating a greater number of active Nd binding sites. Further increasing the dose to 0.15 g/mL raises efficiency to nearly 99% for both resins. This suggests the system is approaching saturation, with most Nd ions having sufficient exchange sites. Beyond 0.20 g/mL, improvements are minimal, with efficiencies stabilizing around 99.4%. This plateau indicates that once enough functional sites are present, adding extra resin does not significantly improve performance. Both Amberlite IRC120 and Dowex G26 show similar patterns, suggesting comparable effectiveness.

Resin with Both Phosphonic and Sulfonic Acid Groups

The adsorption efficiency of Purolite MTS9570, containing both phosphonic and sulfonic acid groups, to Nd and Dy ions from aqueous solutions is shown in Figure 5. At the lowest resin dose (0.05 g/mL), the adsorption of Dy reached 95%, indicating a strong initial interaction between Dy ions and the resin. In contrast, the adsorption efficiency of Nd at the smallest dose (0.05 g/mL) is lower, showing an initial value of 80% compared to Dy. However, as the resin dosage increases to 0.1 g/mL, the adsorption efficiency of Nd^{3+} significantly improves, reaching over 97%. Beyond 0.15 g/mL, the adsorption efficiency plateaus for both Nd and Dy reach over 99% at higher resin dosages, suggesting that equilibrium has been reached and additional resin dosage does not significantly improve Dy and Nd adsorption. Clearly, Purolite MTS9570 is highly effective for adsorbing both Dy and Nd ions from aqueous solutions, with slightly better performance for dysprosium adsorption.

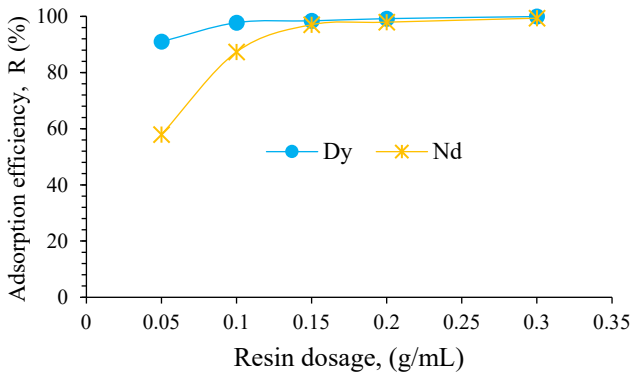


Figure 5. Adsorption efficiency of Purolite MTS9570 with phosphonic and sulfonic acid groups at pH 0.67, 150 rpm, room temperature, and 60 min contact time.

Resin Containing Sulfonic Acid/Trimethylamine Groups

The adsorption behavior of Amberlite IRN-150 resin containing sulfonic acid/trimethylamine groups in the single metal solution of dysprosium (Dy) or neodymium (Nd) ions is illustrated in Figure 6. At a low resin dosage of 0.05 g/mL, the Dy adsorption efficiency is above 72%, while the Nd adsorption value is around 48%. When the resin dosage is increased up to 0.15 g/mL, both Dy and Nd show a significant increase in adsorption efficiency, up to over 94% and 96% for Dy and Nd, respectively. Beyond a dosage of 0.15 g/mL, the adsorption efficiencies of both Dy and Nd maintain plateau values close to 97%, which represents the achievement of the adsorption equilibrium.

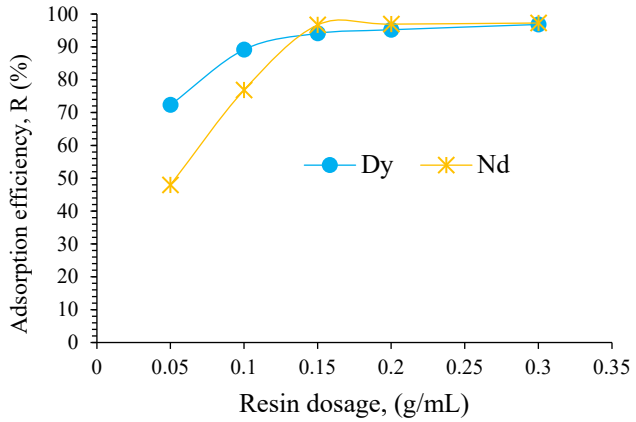


Figure 6. Adsorption using Amberlite IRN-150 resin with sulfonic acid/trimethylamine groups at pH 0.67, 150 rpm, room temperature, and 60 min contact time.

Resin with Aminomethylphosphonic Groups

Figure 7 presents the adsorption percentage of neodymium (Nd) and dysprosium (Dy) ions from single aqueous solutions using Lewatit® MDS TP 260 resin containing an aminomethylphosphonic group at various resin dosages from 0.05 to 0.30 g/mL.

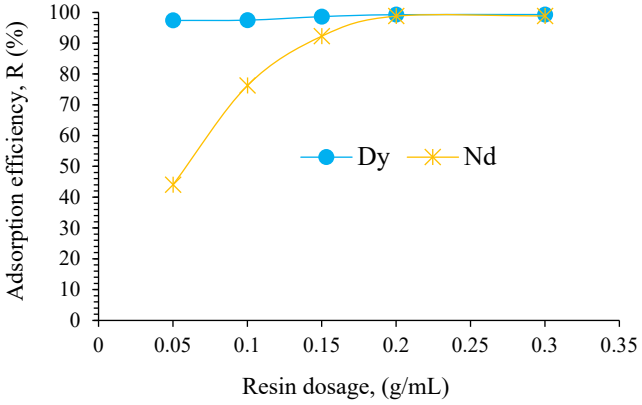


Figure 7. Adsorption using Lewatit MDSTP 260 resin with aminomethylphosphonic acid groups at pH 0.67, 150 rpm, room temperature, and 60 min contact time.

For Dy, the MDS TP 260 resin has an exceptionally high adsorption efficiency, achieving over 97% adsorption at a low resin dosage of 0.05 g/mL. The adsorption efficiency increases by 2%, reaching nearly 100% at the highest resin dosage. In contrast, the adsorption efficiency of Nd starts at 44% with a resin dosage of 0.05 g/mL, then improves dramatically, rising to nearly 99% with a dosage of 0.2 g/mL, where this rise can be due to the increased availability of active binding sites; beyond this point, the adsorption efficiency stabilizes, reaching equilibrium.

It is found that the resins with aminomethylphosphonic acid groups, phosphonic and sulfonic acid groups, sulfonic acid groups, aminophosphonic functional groups, and sulfonic acid/trimethylamine groups have a high adsorption efficiency for Dy at low dosages in single solutions, while Nd requires higher resin dosages to achieve similar efficiencies due to the lower concentration of Dy relative to Nd in single metal solutions.

Resin with Thiol Functional Groups

Figure 8 shows the adsorption performance of Puromet MTS9240 resin containing thiol groups for neodymium (Nd) and dysprosium (Dy) ions in single solutions with a varied resin dosage from 0.05 to 0.30 g/mL.

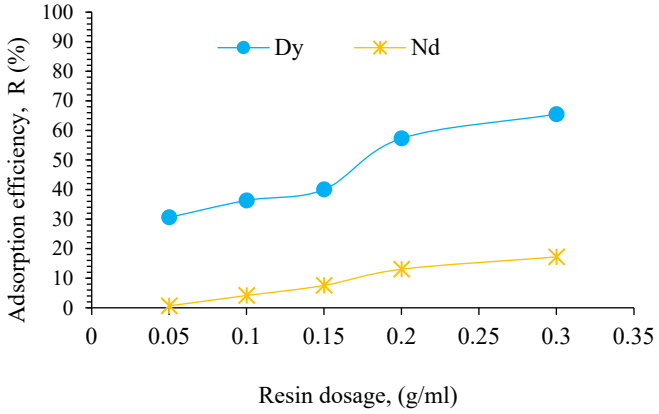


Figure 8. Adsorption using Puromet MTS9240 resin with thiol functional groups at pH 0.67, 150 rpm, room temperature, and 60 min contact time.

At the lowest dosage tested, Dy adsorption efficiency is modest, at about 30%. As resin dosage increases to 0.3 g/mL, Dy adsorption efficiency improves gradually, reaching over 65%, whereas Nd adsorption efficiency started extremely low, close to 0%, and as resin dosage increased to 0.3 g/mL, Nd adsorption efficiency reached only around 18%.

3.2. Resin Adsorption from Nd-Dy Binary Solution

Based on the above experimental findings and our previous study on Nd/Dy separation using Puromet MTX7010 resin impregnated with D2EHPA [14], Puromet MTX7010 resin has demonstrated superior performance, particularly owing to its strong adsorption preference for dysprosium over neodymium. In this work, the effectiveness of D2EHPA as an efficient functional group (ligand) is further evaluated through a comprehensive investigation on the separation and purification of dysprosium and neodymium using another resin impregnated with D2EHPA, i.e., Lewatit® VP OC 1026. The Nd/Dy binary solution was prepared according to the specifications outlined in Section 2.2.

The adsorption tests were conducted using different resin dosages (i.e., 0.05, 0.1, 0.15, 0.2, and 0.3 g/mL) at conditions of pH 0.67, a shaking speed 150 rpm, and a contact time 60 min at room temperature. As shown in Figure 9, at a 0.05 g/mL resin dosage, the adsorption efficiency of Dy^{3+} exceeds 75%, while Nd^{3+} adsorption efficiency is minimal, less than 2%. This remarkable difference in uptake demonstrates the strong affinity of Lewatit® VP OC 1026 for dysprosium ions. This is likely due to the smaller ionic radius and higher charge density of Dy, which make it more strongly bonded to the resin's functional groups, consistent with references [3,33,36]. As the resin dosage increases from 0.1 g/mL to 0.3 g/mL, Dy adsorption continues to rise, exceeding 85% at the maximum resin dosage. In contrast, Nd(III) shows substantially lower adsorption efficiency, increasing gradually from 1.24% to 15.99% over the same dosage range. This pattern suggests that the additional resin mass provides more active binding sites, resulting in increased metal ion–resin contact and higher metal uptake, which enables Nd adsorption. In general, the resin demonstrated a high Dy/Nd selectivity ratio. These results demonstrate the potential for effective separation and purification of neodymium and dysprosium by leveraging the resin's selective affinity, which originated from D2EHPA, and by optimizing operational factors such as solution pH, contact time, agitation speed, and temperature.

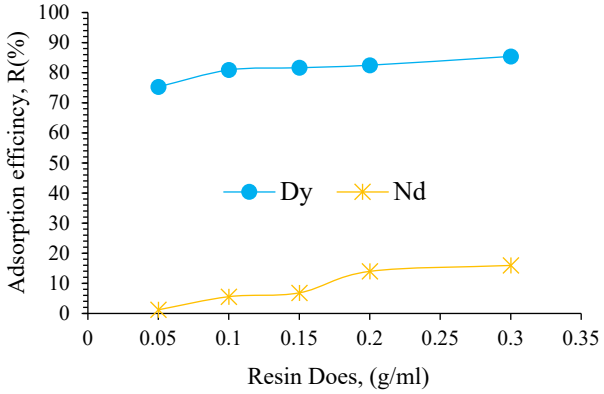


Figure 9. Impact of resin dosage on the adsorption of Nd^{3+} and Dy^{3+} ions at pH 0.67, 150 rpm, room temperature, and 60 min contact time.

3.3. Systematic Study to Optimize Operational Parameters Governing the Separation of Nd^{3+} and Dy^{3+}

3.3.1. Effect of Contact Time

Adsorption tests were conducted over the time range of 5 to 150 min at pH 0.67, resin dosage 0.1 g/mL, and shaking speed 150 rpm at room temperature. As illustrated in Figure 10, a pronounced difference in adsorption efficiency (R%) between Nd and Dy was observed. Dy adsorption efficiency increased sharply within the first 5 min, reaching over 82%, followed by a slight increase reaching near 86% after 150 min. In contrast, Nd showed a much lower adsorption efficiency of 4.20% at 5 min and reached nearly 23% after 150 min. This behavior can be attributed to the stronger affinity of D2EHPA on the resin toward Dy^{3+} ions. The preferential adsorption of dysprosium is likely due to its smaller ionic radius ($Dy^{3+} \approx 0.91$ Å vs. $Nd^{3+} \approx 0.983$ Å) and higher charge density, which enhance electrostatic interactions and promote more stable coordination with the di-(2-ethylhexyl) phosphoric acid (D2EHPA) ligands on the resin [68,69].

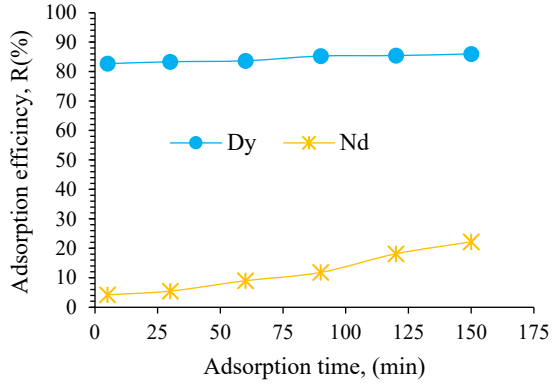


Figure 10. Impact of adsorption time on adsorption efficiencies of Nd^{3+} and Dy^{3+} ions at pH 0.67, 150 rpm, room temperature, and 0.1 g/mL resin dosage.

3.3.2. Effect of pH

The effect of solution pH on the adsorption efficiency of Dy and Nd over a pH range of 0.25 to 2.50 was tested at a contact time of 5 min, resin dosage of 0.1 g/mL, and agitation speed of 150 rpm at room temperature. As shown in Figure 11, both elements showed increased adsorption with higher pH, although their responses varied significantly. Dy^{3+} adsorption was already over 63% at pH 0.25, then increased sharply to over 83% at pH 0.6, and plateaued at 83.23% at pH 2.50. This early saturation indicates that Dy^{3+} binding sites are largely occupied even under strongly acidic conditions. In contrast, Nd^{3+} showed much lower adsorption efficiency throughout the tested pH range. The adsorption of Nd^{3+}

increased gradually from 2.45% at pH 0.25 to 40.16% at pH 2.50 but remained significantly lower than that of Dy^{3+} at all pH values. The increasing trend suggests that higher pH values activate the dissociation of H^+ ions from the resin's active sites, thereby enhancing Nd^{3+} uptake. However, the resin still maintained a pronounced preference for Dy^{3+}; therefore, the optimal pH is near 0.6, where Dy adsorption exceeds 83% and Nd adsorption remains at 4.6%.

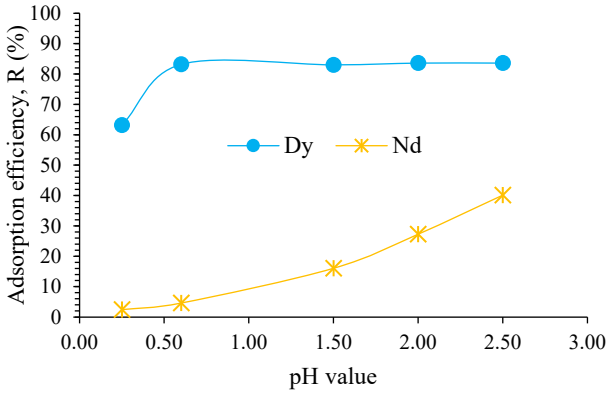


Figure 11. Impact of pH value on adsorption efficiencies of Nd^{3+} and Dy^{3+} ions at 150 rpm, room temperature, 5 min contact time, and 0.1 g/mL resin dosage.

3.3.3. Effect of Shaking Speed

The effect of shaking speed on the adsorption efficiency of Nd^{3+} and Dy^{3+} was investigated at a contact time of 5 min, a resin dosage of 0.1 g/mL, and a solution pH of 0.67 at room temperature. As Figure 12 illustrates, increasing the shaking speed from 0 to 150 rpm significantly enhances Dy^{3+} adsorption, rising from around 35% to over 81%, after which a small improvement is observed up to 200 rpm. This trend indicates that higher agitation speed enhances mass transfer and reduces boundary layer resistance, thereby facilitating faster transport of Dy^{3+} ions to the resin surface.

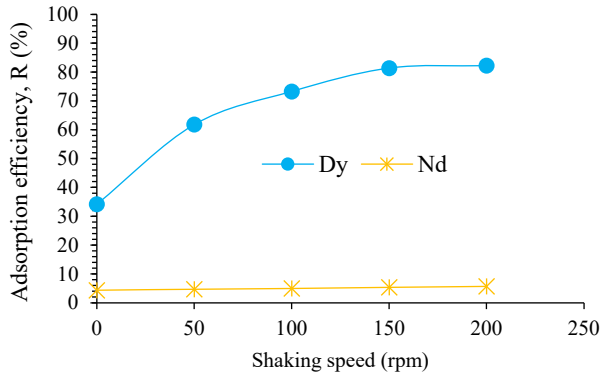


Figure 12. Impact of agitation speed (rpm) on adsorption efficiencies of Nd^{3+} and Dy^{3+} ions at pH 0.67, room temperature, 5 min contact time, and 0.1 g/mL resin dosage.

In contrast, Nd^{3+} adsorption remains consistently low between 4% and 6% across the entire range of shaking speeds, showing minimal sensitivity to agitation. This suggests that Nd^{3+} has a weaker interaction with D2EHPA on the resin and is not significantly influenced by mass transfer improvements.

3.3.4. Impact of Temperature on the Adsorption Efficiencies of Nd^{3+} and Dy^{3+}

A batch of experiments was conducted at 5 min adsorption time, pH 0.67, 150 rpm agitation, and 0.1 g/mL resin dosage to study the effect of temperature on the adsorption

efficiency of Nd^{3+} and Dy^{3+}. As illustrated in Figure 13, Dy^{3+} exhibits consistently high adsorption efficiency across the studied temperature range, increasing slightly from 87.91% at 22 °C to over 89% at 70 °C. In contrast, Nd^{3+} adsorption improved noticeably with temperature, rising from 5.03% at 22 °C to 23.83% at 70 °C.

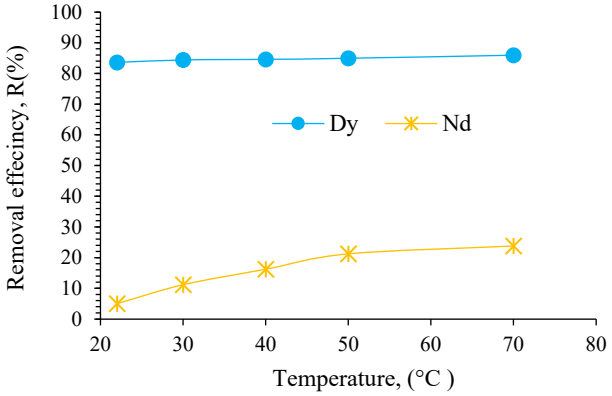


Figure 13. Impact of temperature on adsorption efficiencies of Nd^{3+} and Dy^{3+} ions at pH 0.67, 150 rpm, 5 min contact time, and 0.1 g/mL resin dosage.

Generally, temperature has minimal influence on Dy adsorption. The slight increase of neodymium adsorption efficiency with temperature may be due to the activation and the endothermic property of the Nd adsorption reaction.

4. Effect of Number of Adsorption Stages and Resin Dosage on Nd/Dy Uptake

As illustrated in Figure 9, at a low resin dosage (i.e., 0.05 g/mL), the adsorption efficiency of Dy^{3+} exceeds 75%, while Nd^{3+} adsorption efficiency is barely below 2%, showcasing high adsorption selectivity of the Lewatit® VP OC 1026 resin to Dy^{3+} ions. However, with the increase of resin dosage, the adsorption selectivity to Dy^{3+}decreased due to more active adsorption sites available at the same time. Therefore, it is possible to improve the adsorption selectivity at a high resin dosage by employing a multi-stage adsorption process, i.e., limited resin dosage at each stage, to achieve an ideal separation of Nd^{3+} and $Dy^{3+}$with reasonably high metal recoveries. A series of experiments was conducted with different resin dosages across multiple stages to evaluate the effects of resin dosage and the number of stages on metal adsorption.

Table 4 summarizes the adsorption performance of Lewatit® VP OC 1026 resin to Nd^{3+} and Dy^{3+} at pH 0.67, room temperature, a shaking speed of 150 rpm, and 5 min contact time under different resin dosage and stage number configurations. The results demonstrate that both parameters (i.e., resin dosage and stage number) play a critical role in determining adsorption efficiency and selectivity.

In the one-stage adsorption system, increasing the resin dosage from 0.05 to 0.1 g/mL enhances Dy^{3+} recovery from 70.42% to 80.58%, due to increased availability of active sites. However, this enhancement is accompanied by a rise in Nd^{3+} adsorption from 3.34% to 5.21%, thereby reducing selectivity.

The effect of multi-stage adsorption is pronounced. At a lower total resin dosage of 0.05 g/mL, the two-stage configuration (0.025-0.025 g/mL) achieves 78.95% Dy^{3+} recovery with minimal Nd^{3+} adsorption of 1.79%, whereas it was 70.42% for Dy recovery and 3.34% for Nd^{3+} adsorption under one-stage adsorption, highlighting better selectivity by limited available active sites during adsorption process.

Table 4. Summary of Nd^{3+} and Dy^{3+} adsorption using different stages and different Lewatit® VP OC 1026 resin dosages.

Resin	pH	Time (min)	Nd			Dy	
			Resin Dosage (g/mL)	Conc. (mg/L)	Recovery %	Conc. (mg/L)	Recovery %
Lewatit® VP OC 1026	0.67	5 min	2 stages 0.025-0.025	5672.6	1.79	45.7	78.95
			1 stage 0.05	5583.1	3.34	64.3	70.42
			2 stages 0.05-0.05	5537.1	4.13	26.2	87.95
			3 stages 0.05-0.05-0.05	5437.1	5.87	13.3	92.90
			1 stage 0.1	5474.7	5.21	42.2	80.58
			2 stages 0.1-0.1	5394.3	6.61	21.2	90.25

Increasing both the number of stages and total dosage significantly improves Dy^{3+} recovery. For example, the two-stage system (0.05-0.05 g/mL) increases Dy^{3+} removal to 87.95%, while the three-stage configuration (0.05-0.05-0.05 g/mL) further enhances Dy^{3+} removal to 92.90%. However, this improvement is accompanied by a gradual increase in Nd^{3+} adsorption (up to 5.87%), indicating a trade-off between recovery and selectivity.

Similarly, a two-stage high-dosage system (0.1-0.1 g/mL) achieves 90.25% Dy^{3+} removal but results in the highest Nd^{3+} adsorption (6.61%), suggesting that excessive resin dosage reduces selectivity due to increased co-adsorption of Nd^{3+}.

Overall, at the same total resin dosage, increasing the number of adsorption stages improves Dy^{3+} adsorption selectivity by allowing more competitive occupation of resin active sites across sequential steps. However, increasing the total resin dosage, particularly at higher levels, promotes non-selective adsorption and reduces separation efficiency. Ideal metal separation could be realized by optimizing the resin dosage and stage number configuration.

5. Influence of Acid Concentration and Multi-Stage Elution

After selective adsorption towards dysprosium, the process proceeds to the desorption (elution) stage, which is the reverse of adsorption. This step is essential for recovering the adsorbed metal ions and regenerating the resin for reuse. It uses eluents, such as acids, under various operating conditions [3,14,30].

The elution of Nd and Dy from loaded Lewatit® VP OC 1026 resin was examined using H_2SO_4 with three different concentrations (i.e., 10%, 20%, and 30%) under room temperature in a two-stage eluting process, with each stage lasting 30 min, using the resin samples obtained from the 0.05-0.05-0.05 g/mL resin three-stage adsorption described in Table 4.

As illustrated in Table 5, in the first elution stage, increasing the sulfuric acid concentration significantly enhanced metal recovery. Nd elution efficiency increased from 74.73% at a 10% sulfuric acid concentration to 90.32% at a 30% sulfuric acid concentration, while Dy elution improved from 82.02% to 95.48%, indicating that higher acid concentrations effectively disrupt metal–resin interactions.

Table 5. Elution efficiency of H_2SO_4 at different concentrations and multi-stage elution.

0.05-0.05-0.05 g/mL Dosage of Lewatit® VP OC 1026 and 5 min Contact Time						First Elution Stage for 30 min.					Second Elution Stage for 30 min.			
Nd Conc. (mg/L)	Nd R%	Dy Conc. (mg/L)	Dy R%	Loaded Nd (mg/L)	Loaded Dy (mg/L)	Acid Conc.	Metal Conc. in Eluted Solution		Elution Efficiency		Acid Conc.	Metal Conc. in Eluted Solution		Elution Efficiency	
							Nd (mg/L)	Dy (mg/L)	Nd (%)	Dy (%)		Nd (mg/L)	Dy (mg/L)	Nd (%)	Dy (%)
5437.63	5.86	13.31	92.90	338.21	173.99	10% H_2SO_4	252.75	142.71	74.73	82.02	10% H_2SO_4	85.47	31.28	76.25	82.086
5443.37	5.76	14.11	92.47	332.48	173.18	20% H_2SO_4	263.89	159.11	79.37	91.87	20% H_2SO_4	68.59	14.07	84.90	86.346
5452.13	5.60	15.70	91.62	323.72	171.60	30% H_2SO_4	292.39	163.84	90.32	95.48	30% H_2SO_4	31.33	12.25	87.33	97.973

In the second elution stage, additional recovery of the remaining metals on resin was achieved at this operation. Similar to the first stage elution, higher acid concentrations obtained better metal elution efficiency.

Overall, the results demonstrate that elution efficiency increases with acid concentration in both stages, with the first stage responsible for most of the metal recovery and the second stage providing complementary recovery of residual metals. The eluted resin could be recycled to the adsorption process with a large percentage of available active sites.

6. Multi-Stage Resin Adsorption-Elution Process Analogous to Distillation for Nd and Dy Separation and Purification

As described in Section 2.2, the binary solution contained around 200 mg/L Dy and 6000 mg/L Nd. This substantial concentration disparity between Dy and Nd poses a major challenge to achieving effective purification of Dy, even when highly selective functional groups are employed. According to Table 4, the multi-adsorption process of a 0.05-0.05-0.05 g/mL resin dosage achieved a Dy recovery exceeding 92%. Conversely, Nd adsorption efficiency remained below 6%, but due to its higher concentration in the Nd-Dy solution, it still accounted for a higher concentration than Dy in the elution solution. To address this main challenge, a multistage adsorption-elution process analogous to distillation (e.g., both use repeated cycles to enrich a product, the metal loaded on the resin is analogous to vapor, and the left solution is analogous to heavy oils) will be employed to achieve high separation and purification efficiency by taking advantage of the strong resin affinity for Dy, given the substantial concentration difference [14]. A batch of experiments was conducted to evaluate the multistage adsorption-elution process for separating neodymium and dysprosium using Lewatit® VP OC 1026 resin under optimized adsorption conditions (i.e., pH of 0.67, shaking speed of 150 rpm, temperature at 24 °C, and contact time of 5 min) with varying resin dosages and elution conditions (i.e., 30% H_2SO_4, elution time of 30 min, shaking speed of 150 rpm, room temperature). Figure 14 illustrates the entire sequence of three multi-adsorption stages and two elution stages with the initial 20 mL solution containing 238.843 mg/L Dy and 6246.487 mg/L Nd. The results of Nd and Dy separation and purification via a multistage adsorption-elution process are listed in Table 6.

During the first multi-adsorption stage for Nd purification, resin dosage was reduced stepwise, with 0.1 g/mL (2 g) used in step 1, followed by 0.05 g/mL in step 2, and 0.025 g/mL in step 3. The resulting solution (i) from the first multi-adsorption stage was analyzed, which contained 5896.01 mg/L Nd and 4.10 mg/L Dy, representing a recovery of 94.40% and a prospective purity of 99.93% for Nd in the solution, as shown in Table 6. These

results demonstrate that the multi-adsorption configuration, combined with a progressive reduction in resin dosage, effectively enhances the separation of Nd from Dy.

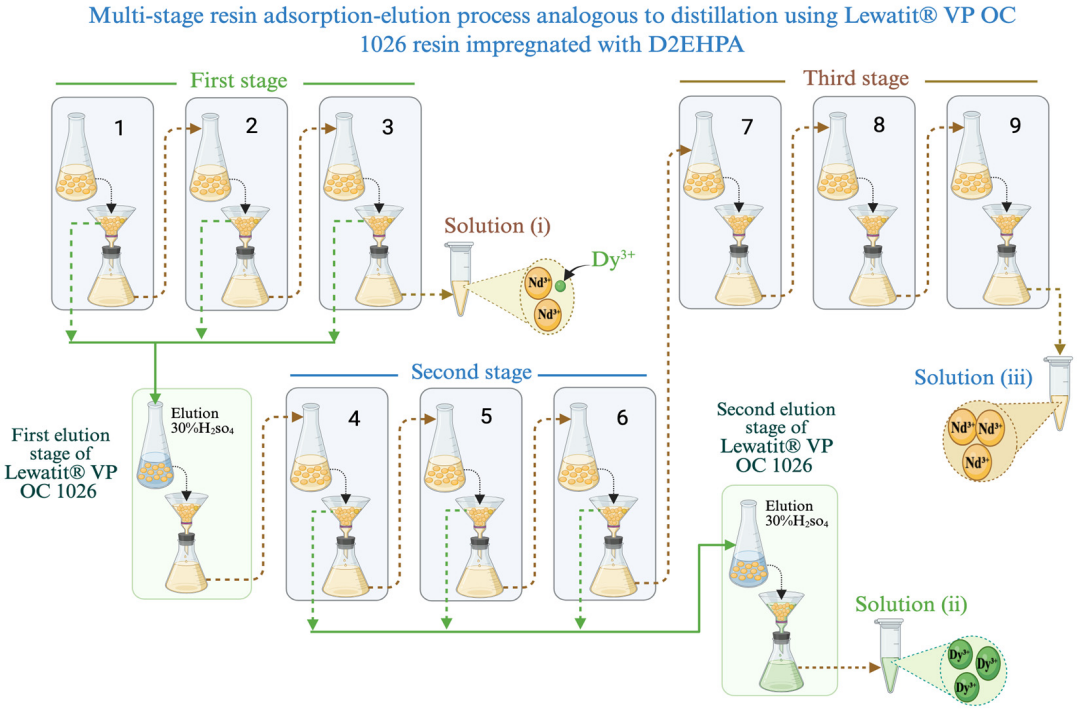


Figure 14. Multi-stage resin adsorption-elution process, analogous to distillation.

Table 6. Separation and purification of Nd and Dy via a multistage adsorption-elution process using Lewatit® VP OC 1026 resin.

Purity of Nd and Dy	Dy Conc. (mg/L)	Nd Conc. (mg/L)	Dy Recovery (%)	Nd Recovery (%)	Dy Purity (%)	Nd Purity (%)
Initial solution	238.843	6246.487	-----	-----	3.67	96.33
Solution i	4.10	5896.01	1.72	94.40	0.07	99.93
Solution ii	231.94	2.03	97.45	0.03	99.13	0.87
Solution iii	0.01	344.79	0.00	5.52	0.0026	99.99

As illustrated in Figure 14, the first elution stage was performed on the resins collected from the adsorption steps 1, 2, and 3 in the first multi-adsorption stage (3.5 g in total) using 20 mL of 30% (*v*/*v*) H_2SO_4 for 30 min. This was followed by the second multi-adsorption stage for Dy purification, which included adsorption steps 4, 5, and 6, with resin dosages of 0.05 g/mL, 0.015 g/mL, and 0.010 g/mL, respectively. The final solution served as input for the third multi-adsorption stage, including steps 7, 8, and 9 for Nd recovery and purification. The total resin collected (1.5 g) from the second multi-adsorption stage was used in the second elution process for Dy recovery, with the same volume and concentration of H_2SO_4 as in the first elution. The obtained solution (ii) was analyzed with 231.94 mg/L Dy and 2.03 mg/L Nd, representing a prospective purity of 99.13% and recovery of 97.45% for Dy. The third multi-adsorption stage consisted of three adsorption steps: 7, 8, and 9, with resin doses of 0.5 g, 0.2 g, and 0.1 g, respectively. The analysis of the final solution (iii), with an Nd concentration of 344.79 mg/L and a Dy concentration of 0.01 mg/L, indicated a prospective purity of Nd above 99.99%.

The proposed process can be extended by further treating solution-i from the first adsorption stage, enabling the production of neodymium with a prospective purity above

99.99%. Likewise, solution-ii may be further refined to yield higher-purity dysprosium. Solution-iii could also be merged with solution-i with a prospective purity over 99.96% and a recovery of above 99.90% for Nd. Overall, the multi-stage adsorption-elution strategy, conceptually analogous to distillation, significantly enhances the separation and purification efficiency of REEs despite substantial concentration disparity between them.

7. Conclusions

Selective resins containing various functional groups (ligands) were explored to realize the efficient recovery and purification of neodymium and dysprosium from their mixed solutions via ion-exchange processes.

The resins with aminomethylphosphonic acid groups, phosphonic and sulfonic acid groups, sulfonic acid groups, aminophosphonic functional groups, and sulfonic acid/trimethylamine groups have a high adsorption efficiency for Dy at low dosages in single solutions, while Nd requires higher resin dosages to achieve similar efficiencies due to the lower concentration of Dy relative to Nd in single metal solutions.

It was found that Lewatit VP OC 1026 resin impregnated with di-(2-ethylhexyl) phosphoric acid (D2EHPA) had a stronger adsorption preference for Dy ions over Nd ions. Dy adsorption efficiency reached over 82%, whereas Nd adsorption efficiency was barely 4.20% at pH 0.67, resin dosage 0.1 g/mL, and shaking speed 150 rpm at room temperature.

Nd and Dy could be efficiently eluted from the loaded resin using dilute H_2SO_4 solutions, which could ensure resin regeneration and recycling in the process.

At the same total resin dosage, increasing the number of adsorption stages improves metal adsorption selectivity by allowing more competitive occupation of limited active sites on the resin across sequential steps. However, increasing the total resin dosage promotes less selective adsorption and reduces separation efficiency. Ideal metal separation could be realized by optimizing the resin dosage and stage number configuration.

By employing a multistage adsorption-elution process analogous to distillation, efficient Dy-Nd separation and purification were realized from their mixed solution, with a prospective purity of 99.13% and recovery of 97.45% for Dy and a prospective purity over 99.96% and recovery above 99.90% for Nd, despite the large concentration disparity between Dy and Nd, where Nd concentration is over 26 times that of Dy.

The research results demonstrate that efficient recovery and purification of metals from their mixed solutions can be achieved with selective resin adsorption processes analogous to distillation despite large concentration differences of the metals, which presents a novel approach for metal recovery and purification.

Author Contributions: F.A.S.M., investigation, data curation, conceptualization, original draft, visualization, review and editing; Y.Z., conceptualization, methodology, review and editing, project administration, supervision, and funding acquisition. All authors have read and agreed to the published version of the manuscript.

Funding: This research was funded by the Natural Sciences and Engineering Research Council of Canada (NSERC) (Grant/Award Number: RGPIN-2023-03921).

Data Availability Statement: Original data available upon request.

Acknowledgments: The authors gratefully acknowledge the financial support of this work by the Natural Sciences and Engineering Research Council of Canada (NSERC) (Grant/Award Number: RGPIN-2023-03921); Sebastian Kommescher and Wilson Humphries for metal analysis; Purolite, An Ecolab Company; and LANXESS Corporation, Liquid Purification Technologies, for supplying free resin samples.

Conflicts of Interest: The authors declare no conflicts of interest.

References

1. Chen, F.; Liu, F.; Liao, C.; Zhang, T.; Wang, H.; Wang, J.; Zhang, J. A novel stepwise process for the recovery of rare earths and gallium from Nd-Fe-B magnets waste. *Sep. Purif. Technol.* **2025**, *367*, 132756. [CrossRef]
2. Ambaye, T.G.; Vaccari, M.; Castro, F.D.; Prasad, S.; Rtimi, S. Emerging technologies for the recovery of rare earth elements (REEs) from the end-of-life electronic wastes: A review on progress, challenges, and perspectives. *Environ. Sci. Pollut. Res.* **2020**, *27*, 36052–36074. [CrossRef] [PubMed]
3. Sharifian, S.; Wang, N.H.L. Resin-based approaches for selective extraction and purification of rare earth elements: A comprehensive review. *J. Environ. Chem. Eng.* **2024**, *12*, 112402. [CrossRef]
4. Yang, Q.; Li, Y.; Li, B.; Duan, P.; Ren, Z.; Zhou, Z. Selective leaching and recovery of neodymium from NdFeB carbonyl residues. *Sep. Purif. Technol.* **2024**, *329*, 125137. [CrossRef]
5. Yao, T.; Geng, Y.; Sarkis, J.; Xiao, S.; Gao, Z. Dynamic neodymium stocks and flows analysis in China. *Resour. Conserv. Recycl.* **2021**, *174*, 105752. [CrossRef]
6. Dushyantha, N.; Batapola, N.; Ilankoon, I.M.S.K.; Rohitha, S.; Premasiri, R.; Abeysinghe, B.; Ratnayake, N.; Dissanayake, K. The story of rare earth elements (REEs): Occurrences, global distribution, genesis, geology, mineralogy and global production. *Ore Geol. Rev.* **2020**, *122*, 103521. [CrossRef]
7. Voncken, J.H.L. SPRINGER BRIEFS IN EARTH SCIENCES The Rare Earth Elements An Introduction. Available online: http://www.springer.com/series/8897 (accessed on 1 July 2026).
8. Zepf, V. An Overview of the Usefulness and Strategic Value of Rare Earth Metals. In *Rare Earths Industry: Technological, Economic, and Environmental Implications*; Elsevier Inc.: Cham, Switzerland, 2015; pp. 3–17. [CrossRef]
9. Liao, C.; Que, L.; Fu, Z.; Deng, P.; Li, A.; Wang, X.; Chen, S. Research Status of Electrolytic Preparation of Rare Earth Metals and Alloys in Fluoride Molten Salt System: A Mini Review of China. *Metals* **2024**, *14*, 407. [CrossRef]
10. Chen, L.; Wu, Y.; Dong, H.; Meng, M.; Li, C.; Yan, Y.; Chen, J. An overview on membrane strategies for rare earths extraction and separation. *Sep. Purif. Technol.* **2018**, *197*, 70–85. [CrossRef]
11. Das, N.; Das, D. Recovery of rare earth metals through biosorption: An overview. *J. Rare Earths* **2013**, *31*, 933. [CrossRef]
12. Venkatesan, P.; Hoogerstraete, T.V.; Hennebel, T.; Binnemans, K.; Sietsma, J.; Yang, Y. Selective electrochemical extraction of REEs from NdFeB magnet waste at room temperature. *Green Chem.* **2018**, *20*, 1065–1073. [CrossRef]
13. Auke, R.O.; Arrachart, G.; Tavernier, R.; David, G.; Pellet-Rostaing, S. Terephthalaldehyde–Phenolic Resins as a Solid-Phase Extraction System for the Recovery of Rare-Earth Elements. *Polymers* **2022**, *14*, 311. [CrossRef] [PubMed]
14. Mohammed, F.A.S.; Zhang, Y. Recovering and Purifying Neodymium and Dysprosium from Simulated Leaching Solution of Spent NdFeB Magnets via Ion Exchange Processes. *Metals* **2026**, *16*, 504. [CrossRef]
15. Takeda, O.; Okabe, T.H. Current Status on Resource and Recycling Technology for Rare Earths. *Metall. Mater. Trans. E* **2014**, *1*, 160–173. [CrossRef]
16. Hoogerstraete, T.V.; Blanpain, B.; Van Gerven, T.; Binnemans, K. From NdFeB magnets towards the rare-earth oxides: A recycling process consuming only oxalic acid. *RSC Adv.* **2014**, *4*, 64099–64111. [CrossRef]
17. Dupont, D.; Binnemans, K. Recycling of rare earths from NdFeB magnets using a combined leaching/extraction system based on the acidity and thermomorphism of the ionic liquid [Hbet][Tf2N]. *Green Chem.* **2015**, *17*, 2150–2163. [CrossRef]
18. Lee, C.H.; Chen, Y.J.; Liao, C.H.; Popuri, S.R.; Tsai, S.L.; Hung, C.E. Selective leaching process for neodymium recovery from scrap Nd-Fe-B magnet. *Metall. Mater. Trans. A Phys. Metall. Mater. Sci.* **2013**, *44*, 5825–5833. [CrossRef]
19. Abrahami, S.T.; Xiao, Y.; Yang, Y. Rare-earth elements recovery from post-consumer hard-disc drives. *Trans. Inst. Min. Metall. Sect. C Miner. Process. Extr. Metall.* **2015**, *124*, 106–115. [CrossRef]
20. Liu, Z.; Zhou, H.; Li, W.; Luo, X.; Wang, J.; Liu, F. Separation and coextraction of REEs and Fe from NdFeB sludge by co-leaching and stepwise precipitation. *Sep. Purif. Technol.* **2022**, *282*, 119795. [CrossRef]
21. Hérès, X.; Blet, V.; Di Natale, P.; Ouaattou, A.; Mazouz, H.; Dhiba, D.; Cuer, F. Selective extraction of rare earth elements from phosphoric acid by ion exchange resins. *Metals* **2018**, *8*, 682. [CrossRef]
22. Xie, F.; Zhang, T.A.; Dreisinger, D.; Doyle, F. A critical review on solvent extraction of rare earths from aqueous solutions. *Miner. Eng.* **2014**, *56*, 10–28. [CrossRef]
23. Liu, C.; Yan, Q.; Zhang, X.; Lei, L.; Xiao, C. A one-pot process based on P44414Cl-HCl aqueous biphasic system for recovering rare earth elements from NdFeB permanent magnet. *Chin. Chem. Lett.* **2022**, *33*, 953–956. [CrossRef]
24. Freire, M.G.; Neves, C.M.S.S.; Marrucho, I.M.; Coutinho, J.A.P.; Fernandes, A.M. Hydrolysis of tetrafluoroborate and hexafluorophosphate counter ions in imidazolium-based ionic liquids. *J. Phys. Chem. A* **2010**, *114*, 3744–3749. [CrossRef] [PubMed]
25. Pimassoni, Y.S.; Lima, M.T.W.D.C.; Yamane, L.H.; Siman, R.R. The recovery of rare earth elements from waste electrical and electronic equipment: A review. *Hydrometallurgy* **2023**, *222*, 106156. [CrossRef]
26. Erust, C.; Akcil, A.; Tuncuk, A.; Deveci, H.; Yazici, E.Y. A Multi-stage Process for Recovery of Neodymium (Nd) and Dysprosium (Dy) from Spent Hard Disc Drives (HDDs). *Miner. Process. Extr. Metall. Rev.* **2021**, *42*, 90–101. [CrossRef]
27. Shamsuri, A.A.; Abdullah, D.K. Ionic liquids: Preparations and limitations. *Makara J. Sci.* **2010**, *14*, 101–106. [CrossRef]

28. Junior, A.B.B.; Vicente, A.D.A.; Espinosa, D.C.R.; Tenório, J.A.S. Recovery of metals by ion exchange process using chelating resin and sodium dithionite. *J. Mater. Res. Technol.* **2019**, *8*, 4464–4469. [CrossRef]
29. Souza, C.; Ferreira, P.A.P.V.S.; Ladeira, A.C.Q. Separation of Rare Earth Elements by Ion Exchange Resin: pH Effect and the Use of Fractionation Column. *Minerals* **2025**, *15*, 821. [CrossRef]
30. El Ouardi, Y.; Virolainen, S.; Mouele, E.S.M.; Laatikainen, M.; Repo, E.; Laatikainen, K. The recent progress of ion exchange for the separation of rare earths from secondary resources—A review. *Hydrometallurgy* **2023**, *218*, 106047. [CrossRef]
31. Judge, W.D.; Azimi, G. Recent progress in impurity removal during rare earth element processing: A review. *Hydrometallurgy* **2020**, *196*, 105435. [CrossRef]
32. Benamor, M.; Bouariche, Z.; Belaid, T.; Draa, M.T. Kinetic studies on cadmium ions by Amberlite XAD7 impregnated resins containing di(2-ethylhexyl) phosphoric acid as extractant. *Sep. Purif. Technol.* **2008**, *59*, 74–84. [CrossRef]
33. Fila, D.; Hubicki, Z.; Kołodyńska, D. Recovery of metals from waste nickel-metal hydride batteries using multifunctional Diphonix resin. *Adsorption* **2019**, *25*, 367–382. [CrossRef]
34. José, L.B.; Ladeira, A.C.Q. Recovery and separation of rare earth elements from an acid mine drainage-like solution using a strong acid resin. *J. Water Process Eng.* **2021**, *41*, 102052. [CrossRef]
35. Virolainen, S.; Repo, E.; Sainio, T. Recovering rare earth elements from phosphogypsum using a resin-in-leach process: Selection of resin, leaching agent, and eluent. *Hydrometallurgy* **2019**, *189*, 105125. [CrossRef]
36. İnan, S.; Tel, H.; Sert, Ş.; Çetinkaya, B.; Sengül, S.; Özkan, B.; Altaş, Y. Extraction and separation studies of rare earth elements using Cyanex 272 impregnated Amberlite XAD-7 resin. *Hydrometallurgy* **2018**, *181*, 156–163. [CrossRef]
37. Yamada, E.; Murakami, H.; Nishihama, S.; Yoshizuka, K. Separation process of dysprosium and neodymium from waste neodymium magnet. *Sep. Purif. Technol.* **2018**, *192*, 62–68. [CrossRef]
38. Kołodyńska, D.; Fila, D.; Hubicki, Z. Evaluation of possible use of the macroporous ion exchanger in the adsorption process of rare earth elements and heavy metal ions from spent batteries solutions. *Chem. Eng. Process.-Process Intensif.* **2020**, *147*, 107767. [CrossRef]
39. Kołodyńska, D.; Hubicki, Z.; Fila, D. Recovery of rare earth elements from acidic solutions using macroporous ion exchangers. *Sep. Sci. Technol.* **2019**, *54*, 2059–2076. [CrossRef]
40. Masry, B.A.E.; Elgoud, E.M.A.; Rizk, S.E. Modeling and equilibrium studies on the recovery of praseodymium (III), dysprosium (III) and yttrium (III) using acidic cation exchange resin. *BMC Chem.* **2022**, *16*, 37. [CrossRef] [PubMed]
41. EElgoud, M.A.; Ismail, Z.H.; Ahmad, M.I.; El-Nadi, Y.A.; Abdelwahab, S.M.; Aly, H.F. Sorption of Lanthanum(III) and Neodymium(III) from Concentrated Phosphoric Acid by Strongly Acidic Cation Exchange Resin (SQS-6). *Russ. J. Appl. Chem.* **2019**, *92*, 1581–1592. [CrossRef]
42. Shokobayev, N.M.; Bouffier, C.; Dauletbakov, T.S. Rare earth metals sorption recovery from uranium in situ leaching process solutions. *Rare Met.* **2015**, *34*, 195–201. [CrossRef]
43. Xiong, C.; He, R.; Pi, L.; Li, J.; Yao, C.; Jiang, J.; Zheng, X. Adsorption of Neodymium(III) on Acrylic Resin (110 Resin) from Aqueous Solutions. *Sep. Sci. Technol.* **2015**, *50*, 564–572. [CrossRef]
44. Purolite Puromet MTS9100. Available online: https://www.purolite.com/product-pdf/mts9100.pdf (accessed on 1 July 2026).
45. SIR-500 Chelating Resin, Styrenic/DVB Macroporous, Sodium Form. Available online: https://files.plytix.com/api/v1.1/file/public_files/pim/assets/30/49/3c/63/633c4930d71dc7000113d8ce/texts/af/8e/94/69/69948eaf8c5f781e0a0dd425/SIR500_pds.pdf (accessed on 1 July 2026).
46. Resins, C. Purolite-S950-L-AMINO-PHOSPHONIC-CHELATING-WASTE-WATER. Available online: https://www.lenntech.com/Data-sheets/Purolite-S950-L.pdf (accessed on 1 July 2026).
47. Purolite S940. Available online: https://www.purolite.com/product-pdf/S940.pdf (accessed on 1 July 2026).
48. Puromet MTS9500. Available online: https://www.purolite.com/product-pdf/MTS9500.pdf (accessed on 1 July 2026).
49. Puromet MTS9570. Available online: https://www.purolite.com/product-pdf/MTS9570.pdf (accessed on 1 July 2026).
50. Dow-Lenntech. Uniform Particle Size Strong Acid Cation Exchange Resin for Specialty Demineralization and Catalyst Applications Product Type Matrix Functional Group DOWEX* G-26 (H) Strong Acid Cation Styrene-DVB, Gel Sulfonic Acid Guaranteed Sales Specifications H + Form. Available online: https://www.lenntech.com/Data-sheets/Dowex-G-26-L.pdf (accessed on 1 July 2026).
51. DuPont™ AmberLite™ IRC120 Na Ion Exchange Resin Gaussian, Gel, Strong Acid Cation Exchange Resin for Industrial Softening Applications. Available online: https://www.dupont.com/content/dam/water/amer/us/en/water/public/documents/en/IER-AmberLite-IRC120-Na-PDS-45-D01246-en.pdf (accessed on 1 July 2026).
52. Lewatit-Lenntech. Lewatit-VP-OC-1026-Resin-Lenntech. Available online: https://www.lenntech.com/Data-sheets/Lewatit-VP-OC-1026-L.pdf (accessed on 1 July 2026).
53. Puromet MTX7010. Available online: https://www.purolite.com/product-pdf/MTX7010.pdf (accessed on 1 July 2026).
54. Lewatit-MDS-TP-260-L-en. Available online: https://www.lenntech.com/Data-sheets/Lewatit-MDS-TP-260-L-en.pdf (accessed on 1 July 2026).

55. Lenntech, H. AMBERLITE^{TM} IRN150 Nuclear Grade Mixed Bed Resin. Available online: www.lenntech.com (accessed on 1 July 2026).
56. Lewatit-Lenntech. Lewatit-TP-272-Resin-Lenntech. Available online: https://www.lenntech.com/Data-sheets/Lewatit-TP-272-L.pdf (accessed on 1 July 2026).
57. Purolite-MTS9300-L. Available online: https://www.lenntech.com/Data-sheets/Purolite-MTS9300-L.pdf (accessed on 1 July 2026).
58. Purolite S930Plus. Available online: https://www.purolite.com/product-pdf/S930PLUS.pdf (accessed on 1 July 2026).
59. Lewatit-Lennetch. Lewatit-MonoPlus-TP-207-Resin-Lenntech. Available online: https://www.lenntech.com/Data-sheets/Lewatit-MonoPlus-TP-207-L.pdf (accessed on 1 July 2026).
60. LEWATIT ® MonoPlus TP 208. Available online: https://www.lenntech.com/Data-sheets/Lewatit-MonoPlus-TP-208-EN-L.pdf (accessed on 1 July 2026).
61. Purolite-Lenntech. PUROLITE® S930 Chelation Resins CHELATING RESIN FOR COPPER REMOVAL. Available online: https://www.lenntech.com/Data-sheets/Purolite-S930-L.pdf (accessed on 1 July 2026).
62. Purolite-MTS9140-L. Available online: https://www.lenntech.com/Data-sheets/Purolite-MTS9140-L.pdf (accessed on 1 July 2026).
63. lewatit-Lenntech. Lewatit-MonoPlus-TP-214-Resin-Lenntech. Available online: https://www.lenntech.com/Data-sheets/Lewatit-MonoPlus-TP-214-L.pdf (accessed on 1 July 2026).
64. SIR-600. Available online: https://files.plytix.com/api/v1.1/file/public_files/pim/assets/30/49/3c/63/633c4930d71dc7000113d8ce/texts/9e/8e/94/69/69948e9e2695110ae6d2b618/SIR600_pds.pdf (accessed on 1 July 2026).
65. Purolite-MTS9200-L. Available online: https://www.lenntech.com/Data-sheets/Purolite-MTS9200-L.pdf (accessed on 1 July 2026).
66. Purolite-MTS9240-L. Available online: https://www.lenntech.com/Data-sheets/Purolite-MTS9240-L.pdf (accessed on 1 July 2026).
67. Dow-Lenntech. DOWEX^{TM} MAC-3 Resin Macroporous Weak Acid Cation Exchange Resin For Water Softening, Dealkalization and Demineralization Applications. Available online: https://www.lenntech.com/Data-sheets/Dowex-MAC-3-L.pdf (accessed on 1 July 2026).
68. Falco, A.; Neri, M.; Melegari, M.; Baraldi, L.; Bonfant, G.; Tegoni, M.; Serpe, A.; Marchiò, L. Semirigid Ligands Enhance Different Coordination Behavior of Nd and Dy Relevant to Their Separation and Recovery in a Non-aqueous Environment. *Inorg. Chem.* **2022**, *61*, 16110–16121. [CrossRef] [PubMed]
69. Shannon, R.D. Revised effective ionic radii and systematic studies of interatomic distances in halides and chalcogenides. *Acta Cryst. A* **1976**, *32*, 751–767. [CrossRef]

Disclaimer/Publisher's Note: The statements, opinions and data contained in all publications are solely those of the individual author(s) and contributor(s) and not of MDPI and/or the editor(s). MDPI and/or the editor(s) disclaim responsibility for any injury to people or property resulting from any ideas, methods, instructions or products referred to in the content.